Angular correlations between heavy ions and α particles in $^{16}O+^{27}Al$ collisions at 87.4 MeV: Evidence of sequential decay of projectilelike fragments

M. Sasagase, M. Sato, S. Hanashima, K. Furuno, Y. Nagashima, Y. Tagishi, S. M. Lee, and T. Mikumo

Institute of Physics and Tandem Accelerator Center, University of Tsukuba, Ibaraki 305, Japan

(Received 27 May 1982)

Angular correlations have been investigated between projectilelike fragments (from Li to O) and α particles in $^{16}O+^{27}Al$ collisions at 87.4 MeV. For C-α and O-α correlations, clear evidence of the sequential α decays of projectilelike fragments was observed at forward angles. In $^{27}Al(^{16}O,^{12}C(g.s.)\alpha)^{27}Al(g.s.)$, the reaction proceeds mainly via the sequential α decay of the excited ^{16}O nucleus at $E_x \cong 10$, 11.6, 13.2, 15.2, 16.2, and 21 MeV. For the O-α case, evidence of the sequential α decay of $^{20}Ne^*$ ($E_x \cong 8.7$, 12.0, and 15.2 MeV) was observed.

[NUCLEAR REACTIONS $^{16}O+^{27}Al$, $E_{lab}=87.4$ MeV; measured $d^2\sigma/d\Omega_{HI}d\Omega_\alpha$, coincidence between O, N, C, B, Li, and α, in-plane and out-of-plane angular correlations, ^{27}Al target.]

I. INTRODUCTION

In the preceding paper by Sato *et al.*,[1] it has been clarified that between light-heavy ions (the *L-L* system), the deep inelastic collisions (DIC) play an important role, even at relatively low energy, say, $\simeq$100 MeV. Moreover, most of the energy spectrum of each emitted particle lies well below the threshold energies of emission of light particles, such as nucleons and alpha particles. In addition, the yields of α particles and of ejectiles attributable to α-particle stripping, e.g., ^{12}C in the case of ^{16}O-induced reactions, are much larger than those of their adjacent nuclei at forward angles. From the systematic feature of cross sections of isotope production, it is concluded that the breakup of the projectile must play an important role when the ejectiles are observed in the very forward direction.

In order to study the reaction mechanism of DIC, several authors[2] measured the angular correlations between projectilelike heavy ejectiles and α particles. Correlations between heavy fragments and α particles are also of interest from a theoretical point of view.[3]

Angular correlations between C and α particles have been studied, with the same system $^{16}O+^{27}Al$, by Harris *et al.* at 65 MeV (Ref. 4) and 100 MeV,[5] and by Tsang *et al.* at 65 MeV.[6] The results of Harris *et al.* at 65 MeV show that the correlations between ^{12}C at $\theta_{lab}=30°$, near $\theta_{gr}\simeq 24°$, and α particles for the

$$^{27}Al(^{16}O,^{12}C(g.s.)\alpha)^{27}Al(g.s.)$$

reaction indicate the sequential decay of the excited ^{31}P ($E_x \simeq 14.5$ MeV) as the main reaction process. Harris *et al.* also made measurements of the C-α correlation at 100 MeV, with the C detector set at $\theta_{lab}=30°$, well behind θ_{gr} ($\simeq 13°$). The results suggest also the emission of α particles from $^{31}P^*$ and are interpreted as due to the rotation of the dinuclear system (DNS) and the subsequent α decay from the surface of the recoil nucleus, while the projectilelike fragment is still in the vicinity. In contrast, Tsang *et al.* showed that, at the same incident energy of 65 MeV, a small portion of α particles from the breakup of $^{16}O^*$ was detected around the C detector placed at $\theta_{lab}=30°$.

On the other hand, it is well known that most of the total reaction cross section for the $^{16}O+^{27}Al$ collision is attributed to the fusion cross section in the energy range of $E_{lab} \lesssim 65$ MeV.[7,8] Above this energy, the cross sections for DIC increase,[1,7-9] and one of the most remarkable characteristics of these DIC's is expressed by the forward-peaked or exponential angular distribution. Therefore, it is expected, in the present study at 87.4 MeV, that a different reaction mechanism from that at 65 MeV may be obtained. Setting the detectors for heavy ejectiles (HI) at $\theta_{lab}=20°$ and 30°, near and well behind the grazing angle, $\theta_{gr}\simeq 17°$, and identifying their atomic numbers Z ($8 \geq Z \geq 3$), we measured both the in-plane and the out-of-plane HI-α angular correlations. A better energy resolution than in the

measurements by other authors,[4–6] enabled us to demonstrate the evidence of the sequential decay of the projectile and projectilelike nuclei.

II. EXPERIMENTAL PROCEDURE

The experiment was performed using a beam of 88 MeV $^{16}O^{7+}$ ions produced by the 12 UD Pelletron at the Tandem Accelerator Center of the University of Tsukuba. The experimental setup was very similar to that described in the preceding paper.[1] The beam was collimated by the use of a set of three tantalum apertures, consisting of two defining slits $S1$ and $S2$, and an antiscattering slit B. The apertures $S1$ and $S2$ were of 3 and 2 mm diam, respectively. They were 850 mm apart from each other. The aperture B of 3 mm diam was 100 mm distant from $S2$ and 25 mm from a target. The beam intensity was 20—80 nA on the target. Self-supporting aluminum foils of about 400 $\mu g/cm^2$ thickness were used as the target. The mean energy loss of the incident oxygen ions in the target is about 650 keV, so that the mean incident energy is 87.35 MeV.

Conventional ΔE-E counter telescope systems, consisting of Si surface barrier detectors, were used to detect and identify emitted heavy ions (HI, $3 \leq Z \leq 8$) and α particles. For the HI counter telescope, a 16.9 μm thick ΔE detector and a 1000 μm E detector were used. In order to detect α particles, a counter telescope consisting of a 49.5 μm thick ΔE detector and a 2000 μm thick E detector was used at forward angles ($\theta_\alpha < 20°$), while another counter telescope consisting of a 6.7 μm thick ΔE detector and a 1000 μm thick E detector was used at backward angles ($\theta_\alpha \geq 20°$). An aluminum absorber of 80 μm thickness was placed in front of the ΔE detector of the α counter to stop the elastically scattered ^{16}O ions at $\theta_\alpha < 20°$.

Heavy ions were detected at a fixed angle, $\theta_{HI} = 20°$, with a solid angle of 2.3 msr, and coincident α particles were measured by movable α counters with solid angles of 1.4—3.5 msr.

In-plane and out-of-plane correlations were measured for $\theta_{HI} = 20°$. During the in-plane measurements, α particles were detected within the angular range of 5°—110° on both sides of the beam axis in the reaction plane defined by the beam axis and the HI counter.

Hereafter, we define $\theta > 0$ as the side of the HI detector in the case of in-plane correlations. The out-of-plane measurements were done at fixed $\theta_{HI} = 20°$, $\theta_\alpha = 10°$ and 50°, and $\phi_\alpha = 30°$, 60°, and 90°. The azimuthal angle, θ_α, of the α counter is defined as $\phi = 180°$ when it is placed at the same side as that of the HI counter relative to the beam direction. The scattering chamber with alpha detectors was rotated around the beam direction, while the HI detector was set fixed to an auxiliary chamber. In-plane measurements were also done for $\theta_{HI} = 30°$, with a smaller angular range of θ_α than in the case of $\theta_{HI} = 20°$.

Five coincidence signals, namely, ΔE and E signals of the heavy-ion counter, those of the two α counters, and time signals were sent to on-line PDP 11/40 and 11/50 computer systems, and finally recorded event by event on magnetic tape. Using a thinner target and smaller solid angles for both HI and α detectors, we obtained a better energy resolution than that obtained by other authors.[4–6] (See, for instance, Fig. 4.)

III. EXPERIMENTAL RESULTS

A. In-plane and out-of-plane angular correlations

The in-plane and out-of-plane angular correlations between α particles and HI ($3 \leq Z \leq 8$) were measured for $\theta_{HI} = 20°$. The results of the in-plane angular correlation are shown in Figs. 1(a) and (b). For all HI, the correlation shows a peak at forward angles on the opposite side of the heavy-ion counter, i.e., $\theta_\alpha < 0$. As described later for the C-α and O-α cases, the sequential α decays of projectilelike fragments contribute mainly at forward angles.

The out-of-plane angular correlations are presented in Fig. 2. The coincident yields are normalized to the in-plane yields at $\phi_\alpha = 0$. Out-of-plane dependences for both $\theta_\alpha = 10°$ and 50° are very similar to one another, and a strong in-plane correlation was obtained.

From these results, the ratios of the coincident yields to the singles yields were estimated by integrating the angular correlations. We define the α multiplicity, M_α, as

$$M_\alpha = \int \frac{d^2\sigma/d\Omega_{HI}d\Omega_\alpha}{d\sigma/d\Omega_{HI}} d\Omega_\alpha \,. \tag{1}$$

The results obtained are $M_\alpha(O) \simeq 0.6$, $M_\alpha(N) \simeq 0.3$, $M_\alpha(C) \simeq 0.6$, and $M_\alpha(B) \simeq 0.6$. The errors are estimated to be about 20%, although that may be an overestimation by about 50% for the case of $M_\alpha(O)$.

In-plane correlations for $\theta_{HI} = 30°$ were also measured. The results are presented in Fig. 3. In contrast to the case of $\theta_{HI} = 20°$, the remarkable enhancement of coincident yields at forward angles disappears and no preferential direction for α particles is seen.

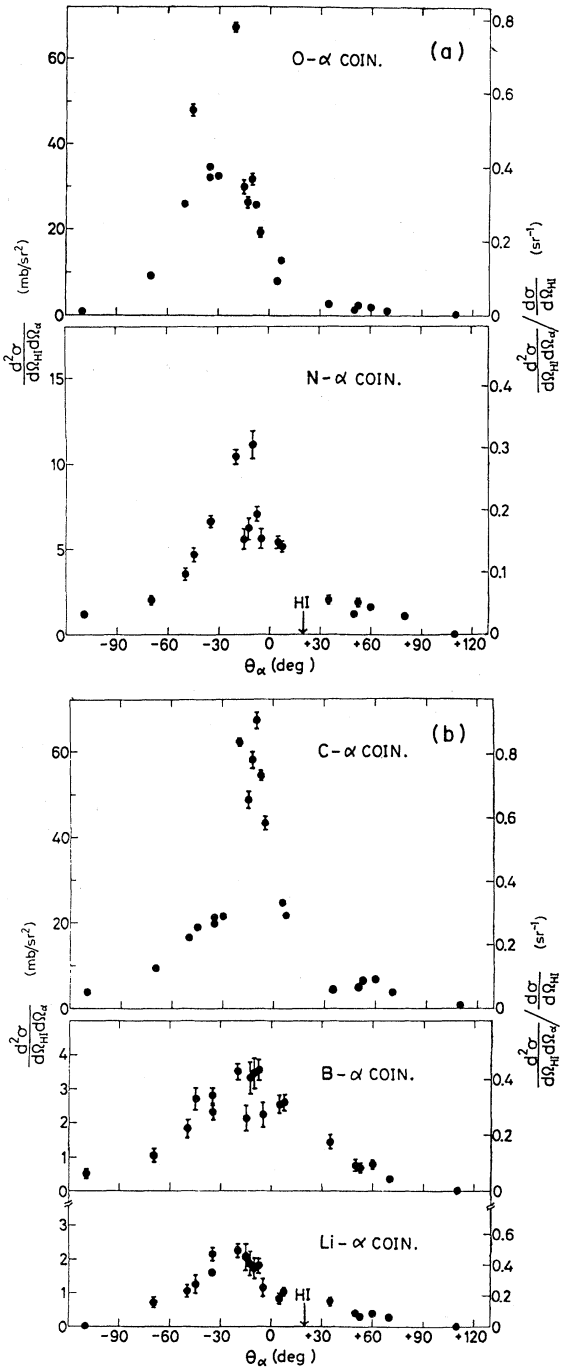

FIG. 1. In-plane angular distributions of α particles coincident with heavy-ions HI (O, N, C, B, Li) measured at $\theta_{HI}=20°$, and the ratio of coincident to singles cross sections. (a) O-α and N-α coincidences (b) C-α, B-α, and Li-α coincidences.

B. Correlation betwen C and α

For the C-α correlation, some remarkable features concerning the reaction mechanism were obtained.

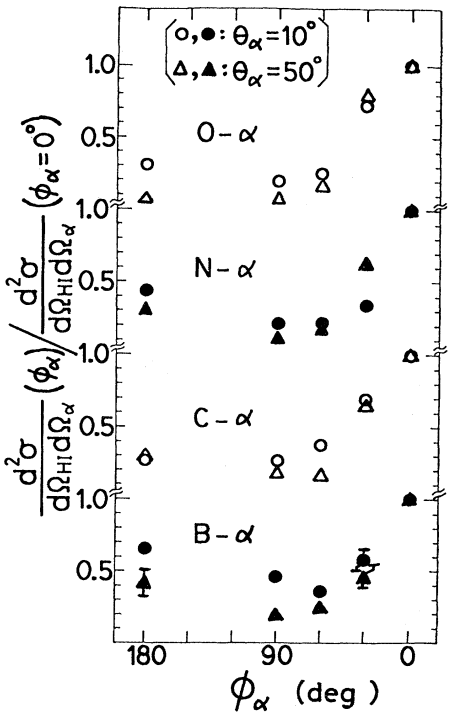

FIG. 2. Out of plane angular distributions of α particles coincident with heavy-ions HI (O, N, C, B). The yields of α particles coincident with HI are normalized to the in-plane yields at $\theta_\alpha=0°$ and $\phi_\alpha=180°$ corresponding to the α counter set at the same side as that of the HI counter seen from the beam. For $\phi_\alpha=180°$ and $\theta_\alpha=10°$, the values were obtained by interpolating the measured in-plane angular distributions.

A Q-value spectrum of C-α coincidence yields at $\theta_C=20°$ and $\theta_\alpha=-7.5°$ is shown in Fig. 4. The Q values were obtained using three-body kinematics and assuming that all C events can be attributed to

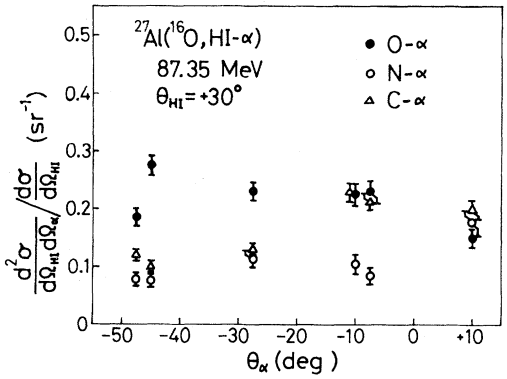

FIG. 3. In-plane angular distributions of α particles coincident with heavy-ions HI (O, N, C) measured at $\theta_{HI}=30°$, expressed by the ratio of coincident to singles cross sections.

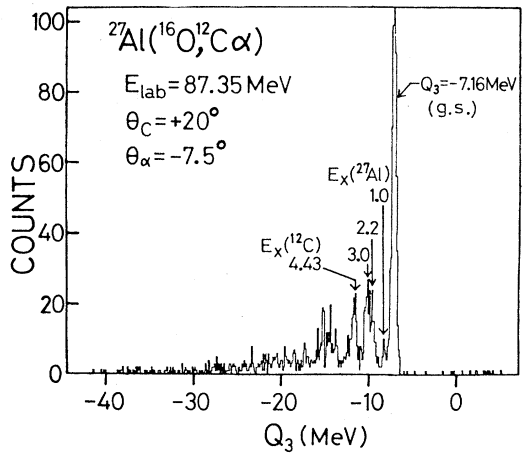

FIG. 4. Q-value spectrum of C-α coincidence yields at $\theta_C=20°$, $\phi_C=180°$, $\theta_\alpha=7.5°$, and $\phi_\alpha=0°$, obtained using the three-body kinematics.

^{12}C. Some final states corresponding to ^{12}C(g.s.)+α+^{27}Al(g.s.), ^{12}C(g.s.)+α+^{27}Al (2.2, 3.0 MeV), and ^{12}C (4.43 MeV)+α+^{27}Al(g.s.) are observed. The final states of ^{12}C(g.s.)+α+^{27}Al(g.s.) are the most clearly seen. The resolution of the Q-value spectrum is found to be about 500 keV in FWHM for this final state. The angle-integrated yield of this final state was about 10% of the total coincident yield. The angular distribution of the yield of α particles coincident with C corresponding to this final state is shown in Fig. 5. The coincident yields are well concentrated at $\theta_\alpha \simeq -10°$ and decrease rapidly with the change of θ_α.

1. *Final states corresponding to* $^{12}C(g.s.)+\alpha+^{27}Al(g.s.)$

The energy spectra of C coincident with α particles corresponding to these ground states are shown in Fig. 6 together with the singles C spectrum. The coincident events were mainly observed in the low energy region of the singles spectrum. Several peaks were observed, and, as will be discussed later, this fact suggests that sequential processes play an important role in this reaction.

As possible sequential processes, the following three types of three-body reactions are taken into account:

$$^{16}O+^{27}Al\rightarrow{}^{16}O^*+^{27}Al\rightarrow{}^{12}C+\alpha+^{27}Al\,, \quad (2)$$

$$^{16}O+^{27}Al\rightarrow{}^{12}C+^{31}P^*\rightarrow{}^{12}C+\alpha+^{27}Al\,, \quad (3)$$

$$^{16}O+^{27}Al\rightarrow\alpha+^{39}K^*\rightarrow\alpha+^{12}C+^{27}Al\,. \quad (4)$$

If the reaction proceeds via process (2), the kinetic energy of relative motion of ^{12}C and the α particle, $E_{C\text{-}\alpha}$, deduced from the peaks, should be independent of θ_α. Similarly, if the reaction proceeds via process (3) or (4), $E_{\alpha\text{-Al}}$ or $E_{C\text{-Al}}$, respectively, should

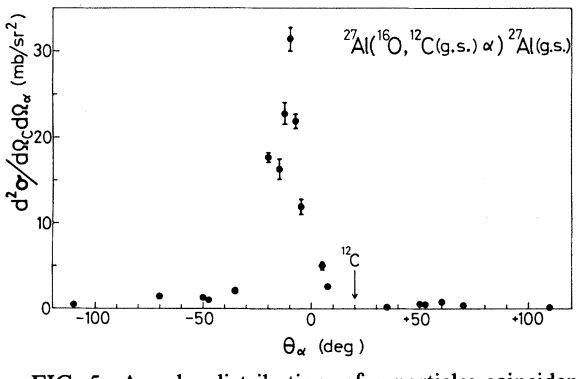

FIG. 5. Angular distributions of α particles coincident with ^{12}C measured at 20°, corresponding to the final state of ^{12}C(g.s.)+α+^{27}Al(g.s.).

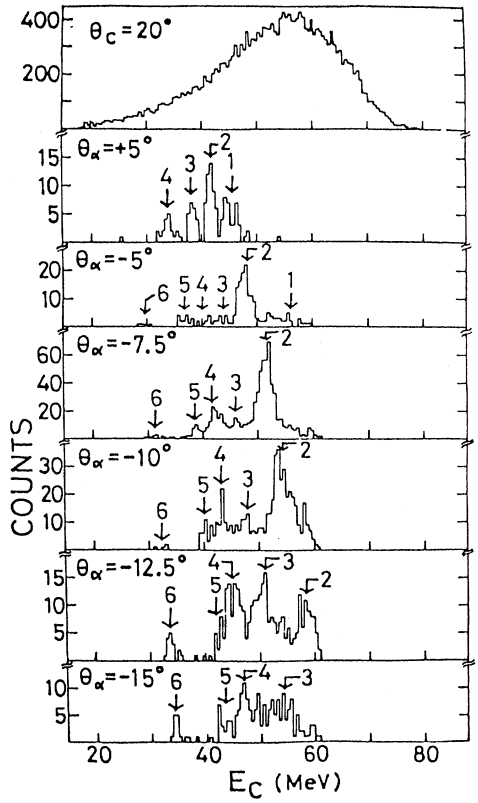

FIG. 6. Singles energy spectra of C (top of the figure) and energy spectra of ^{12}C coincident with α particles corresponding to the final state of ^{12}C(g.s.)+α+^{27}Al(g.s.) obtained at $\theta_C=20°$ and $\phi_C=180°$, and at various θ_α. Labeled numbers correspond to the same relative energies $E_{C\text{-}\alpha}$ and the resultant excitation energies in ^{16}O are given in Table I.

be independent of θ_α. The kinetic energies of relative motion between two particles from the intermediate systems corresponding to the peak labeled as 2 in Fig. 6 are plotted in Fig. 7 as a function of θ_α. The value of $E_{C\text{-}\alpha}$ is independent of θ_α. Therefore, this peak corresponds to process (2). The same conclusion is obtained also for the other labeled peaks in Fig. 6.

We can thus conclude that the

$$^{27}\mathrm{Al}(^{16}\mathrm{O},^{12}\mathrm{C}(\mathrm{g.s.})\alpha)^{27}\mathrm{Al}(\mathrm{g.s.})$$

reaction proceeds mainly via the sequential α decay of the excited ^{16}O nucleus. The value of the relative energies $E_{C\text{-}\alpha}$ and resultant excitation energies in ^{16}O corresponding to the six peaks shown in Fig. 6 are listed in Table I. The peaks seen in the spectra have the widths of about 2–3 MeV, which are mainly due to the kinematical effects. Therefore, a precise determination of the excitation energy of the intermediate states is difficult, but it is sufficient to discriminate among processes (2)–(4).

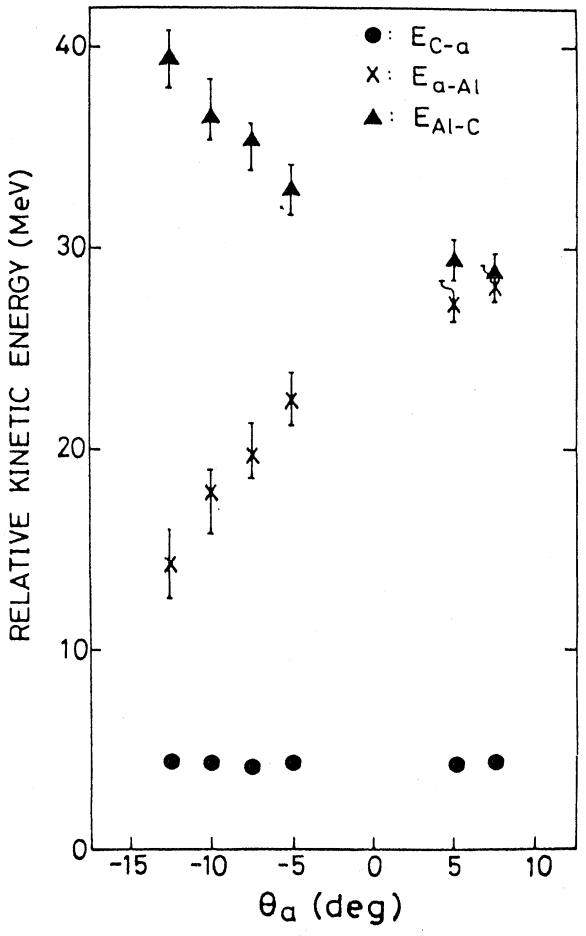

FIG. 7. Kinetic energies of relative motion between two particles from the intermediate systems corresponding to the peak labeled as 2 in Fig. 6 plotted as a function of θ_α. Three possible systems are given in Eqs. (2)–(4), e.g., $^{16}\mathrm{O}^*\rightarrow{}^{12}\mathrm{C}+\alpha$, $^{31}\mathrm{P}^*\rightarrow\alpha+{}^{27}\mathrm{Al}$, and $^{39}\mathrm{K}^*\rightarrow{}^{27}\mathrm{Al}+{}^{12}\mathrm{C}$. Error bars come mainly from kinematical effects of angular resolution, and those for the process $^{16}\mathrm{O}^*\rightarrow{}^{12}\mathrm{C}+\alpha$ are within the filled circles.

Several possible candidates for α-decaying states in ^{16}O exist in the observed energy region. According to Suzuki,[10] probable candidates of ^{12}C-α cluster states in $^{16}\mathrm{O}^*$ with large α_0 widths, Γ_{α_0}, decaying to the ground state of ^{12}C are those at $E_x(J^\pi,\Gamma_{\alpha_0})=9.60(1^-,510)$, $10.35(4^+,27)$, $11.52(2^+,74)$, $11.63(3^-,800)$, $13.02(2^+,150)$, $13.13(3^-,90)$, $14.68(5^-,700)$, $14.82(6^+,28)$, $16.23(6^+,490)$, and $21.01(7^-,750)$, where E_x and Γ_{α_0} are in units of MeV and keV, respectively.

2. *Final states including excited states of ^{27}Al and/or ^{12}C*

As for other final states which include excited states of ^{27}Al and/or ^{12}C, the relative energies, $E_{C\text{-}\alpha}$, $E_{\alpha\text{-Al}}$, and $E_{C\text{-Al}}$ were calculated from the coincident data event by event. As in the case of $^{12}\mathrm{C}(\mathrm{g.s.})+\alpha+{}^{27}\mathrm{Al}(\mathrm{g.s.})$, the enhancement of the coincident yield at energies corresponding to $E_{C\text{-}\alpha}\simeq 4.4$, 6.0, and 8.0 MeV were observed, as shown in Fig. 8. These enhancements were observed at forward alpha angles ($\theta_\alpha \lesssim 20°$), and also at backward angles on the same side as that of the HI counter relative to the beam axis ($\theta_\alpha \gg 0$), as are shown in Figs. 8 and 9, respectively. At backward angles on the opposite side of the HI counter ($\theta_\alpha \ll 0$), the α particles emitted from $^{16}\mathrm{O}^*$ of $E_x \lesssim 20$ MeV cannot be detected for the kinematical reason. In the region of large θ_α, other processes like the sequential α decay of $^{31}\mathrm{P}^*$

TABLE I. Relative energies $E_{C\text{-}\alpha}$ and resultant excitation energies E_x of intermediate projectilelike states in $^{16}\mathrm{O}+{}^{27}\mathrm{Al}\rightarrow{}^{16}\mathrm{O}^*\rightarrow{}^{12}\mathrm{C}(\mathrm{g.s.})+\alpha+{}^{27}\mathrm{Al}(\mathrm{g.s.})$.

$E_{C\text{-}\alpha}$ (MeV)	E_x (^{16}O) (MeV)	Labeled number in Fig. 6
2.8	10.0	1
4.4	11.6	2
6.0	13.2	3
8.0	15.2	4
9.0	16.2	5
14	21.2	6

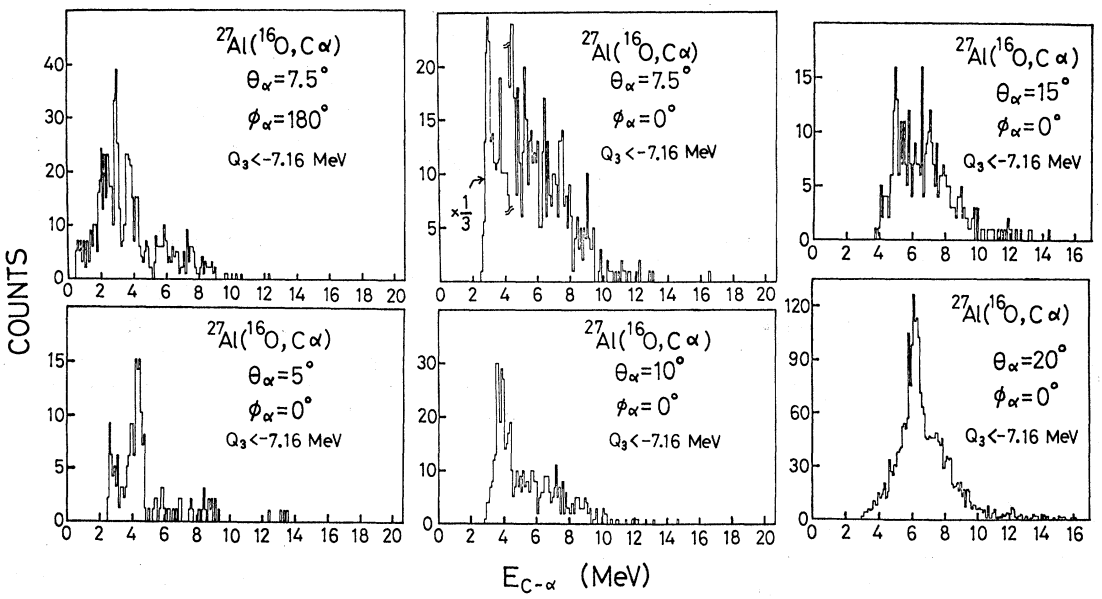

FIG. 8. Spectra of relative energies $E_{C-\alpha}$ for the reaction ^{27}Al(^{16}O,Cα), excluding the final state of ^{12}C(g.s.)+α+^{27}Al(g.s.). θ_C=20° and ϕ_C=180°.

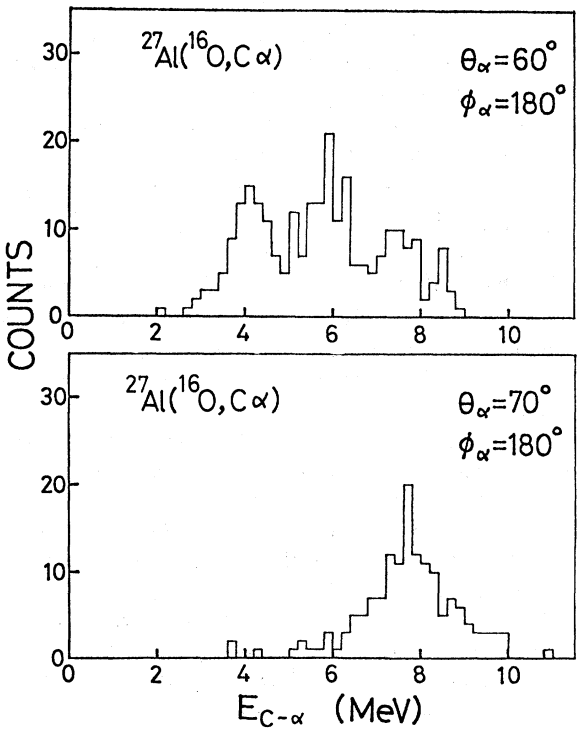

FIG. 9. Spectra of relative energies $E_{C-\alpha}$ for the reaction ^{27}Al(^{16}O,Cα), including all final states at θ_C=20° and ϕ_C=180°. Alpha counters are set at backward angles on the same side of the HI counter relative to the beam direction.

would make a main contribution. Indeed, the spectra of $E_{\alpha\text{-Al}}$ at $\theta_\alpha \gtrsim 45°$ show a broad bump peaked at $E_{\alpha\text{-Al}} \sim 6.5$ MeV, as is shown in Fig. 10. The contribution of the α decays of ^{31}P* is considered to be larger in this region.

C. Correlation between O and α

The correlation between O and α particles gives also some information about the reaction mechanism. A Q-value spectrum of O-α coincidence yields at θ_0=20° and θ_α=−7.5° is shown in Fig. 11, which was obtained assuming that all oxygen events be attributed to ^{16}O. In order to investigate the reaction mechanism, the data were transformed into relative energies as in the case of C-α coincidences.

If the reaction proceeds via a sequential process, the following three processes are possible:

$$^{16}\text{O}+^{27}\text{Al}\rightarrow{}^{20}\text{Ne}^*+{}^{23}\text{Na}\rightarrow{}^{16}\text{O}+\alpha+{}^{23}\text{Na}\ , \quad (5)$$

$$^{16}\text{O}+^{27}\text{Al}\rightarrow{}^{16}\text{O}+{}^{27}\text{Al}^*\rightarrow{}^{16}\text{O}+\alpha+{}^{23}\text{Na}\ , \quad (6)$$

$$^{16}\text{O}+^{27}\text{Al}\rightarrow\alpha+{}^{39}\text{K}^*\rightarrow\alpha+{}^{16}\text{O}+{}^{23}\text{Na}\ . \quad (7)$$

From the analysis of the relative energies, a striking feature suggests the dominance of the sequential α decay of excited ^{20}Ne nuclei at forward angles of θ_α. The spectra of relative energies between ^{16}O and α particles, $E_{O\text{-}\alpha}$, are presented in Fig. 12. Some peaks were observed in the spectra at θ_α near the HI counter. From the similar kinematical consideration

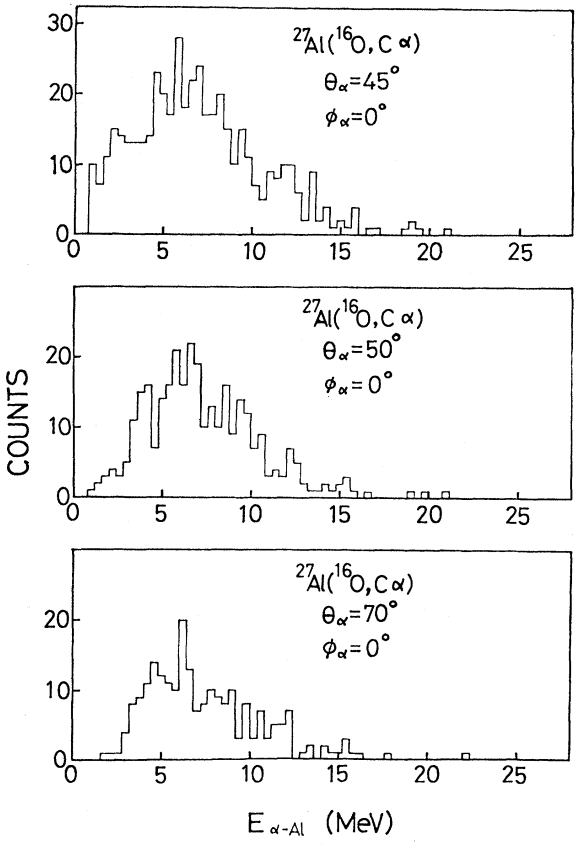

FIG. 10. Spectra of relative energies $E_{\alpha\text{-Al}}$ for the reaction ^{27}Al(^{16}O,Cα), including all final states, $\theta_C=20°$ and $\phi_C=180°$. Alpha counters are set at backward angles on the opposite side of the HI counter relative to the beam direction.

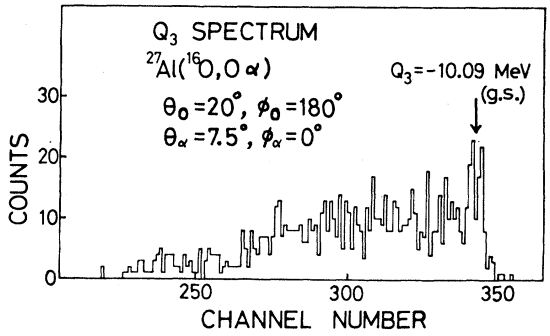

FIG. 11. Q-value spectrum of O-α coincidence yields at $\theta_O=20°$, $\phi_O=180°$, $\theta_\alpha=7.5°$, and $\phi_\alpha=0°$, obtained using the three-body kinematics.

as in the C-α case, these peaks are considered to be due to the sequential α decay of ^{20}Ne*. The values of the relative energies $E_{O\text{-}\alpha}$ and the corresponding excitation energies of ^{20}Ne for the final state of ^{16}O(g.s.)+α+^{23}Na(g.s.) are listed in Table II.

The determination of the reaction mechanism at backward angles of θ_α was rather difficult, since the sequential α decays of ^{27}Al* probably make a large contribution. However, other processes, e.g., the direct three-body breakup process, cannot be excluded.

IV. DISCUSSION

From the present experiment at $E_{lab}=87.4$ MeV, it has been clearly seen that the angular correlations between α particles and heavy-ion products ($\theta_{HI}=20°$) show peaks at forward angles [$\theta_\alpha\simeq-(10°-20°)$]. This feature was shown for the C-α and O-α cases in detail. It is also clarified that the sequential α decay of projectilelike fragments gives a large contribution to the reaction mechanism when α particles are detected at forward angles.

Now, consider, for example, the kinematics of the following process:

$$^{16}\text{O}+^{27}\text{Al}\rightarrow{}^{16}\text{O}^*(E_x=11.6\text{ MeV})+^{27}\text{Al(g.s.)}$$
$$\rightarrow{}^{12}\text{C(g.s.)}+\alpha+^{27}\text{Al(g.s.)}\,. \quad (8)$$

The C-α coincident yield attains the maximum at $\theta_\alpha=10°$ and $\phi_\alpha=0°$, and the contribution from the 11.6 MeV state of ^{16}O* is the largest at this angle. The velocity diagrams of the process are shown in Fig. 13. When an α particle is detected at $\theta_\alpha=10°$ and $\phi_\alpha=0°$, as is shown in Fig. 13(a), the intermediate ^{16}O* nucleus is emitted at $\theta^{c.m.}_{^{16}O^*}\sim20°$ and $\phi^{c.m.}_{^{16}O^*}=180°$ in the c.m. system. The α particle is emitted at $\theta^R_\alpha=0°$ for the direction of the velocity of ^{16}O* in the center of mass system of ^{16}O*. On the other hand, if $\theta_\alpha=5°$ and $\phi_\alpha=180°$, ^{16}O* is emitted at $\theta^{c.m.}_{^{16}O^*}\sim25°$ and $\theta^{c.m.}_{^{16}O^*}=180°$. Then the α particle is emitted at $\theta^R_\alpha\sim43°$, as is shown in Fig. 9.

There are three factors which determine the coincident yield. The first factor is the angular distribution of the primary product ^{16}O*. The second is the transformation coefficient of the solid angles between the laboratory system and the "sequential-decay"-relative-coordinate system. The last one is the angular distribution of α particles in the center of mass system of ^{16}O*.

The angles $\theta_\alpha=10°$ and $\phi_\alpha=0°$ are favored in the second factor and may also be favored in the first factor, since the primary ^{16}O* is emitted at the most forward angle. Beyond $\theta_\alpha=12°$ and $\phi_\alpha=0°$, the α particles decaying from the 11.6 MeV state of ^{16}O* become undetectable. Thus, the coincident yield can exhibit the maximum at $\theta_\alpha=10°$ and $\phi_\alpha=0°$, corresponding to $\theta_\alpha=-10°$ in Figs. 1 and 5.

The enhancement of the coincident yields at forward angles reflects these conditions of the kinemat-

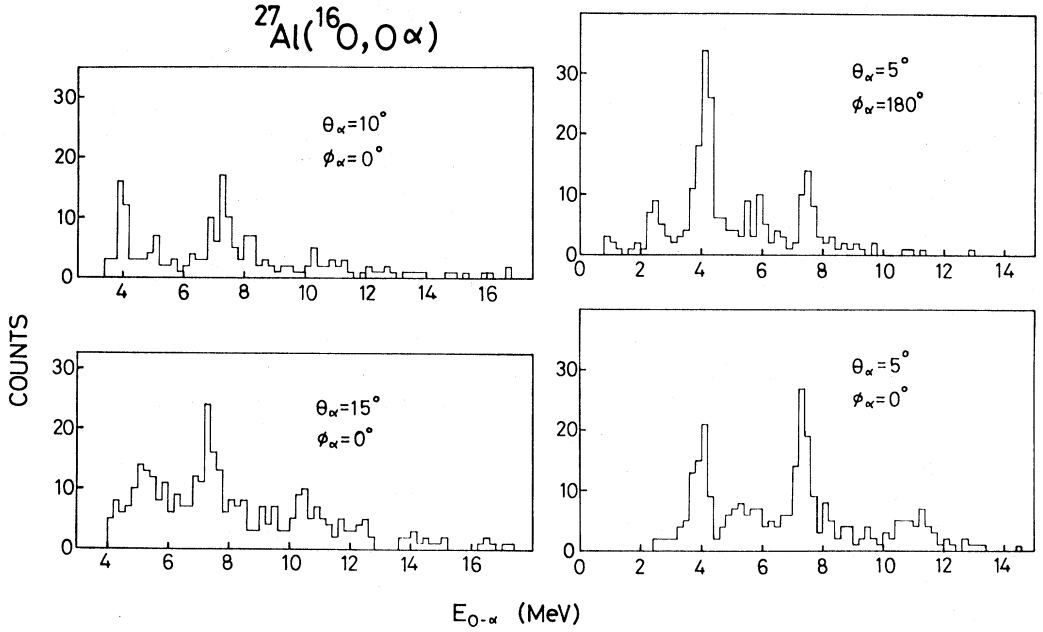

FIG. 12. Spectra of relative energies $E_{O\text{-}\alpha}$ for the reaction ^{27}Al(^{16}O,Oα), including all final states $\theta_O=20°$ and $\phi_O=180°$.

ics. If the excitation energies of the intermediate states are different, the favored kinematical conditions should be different. For example, the contribution from the 15.2 MeV state of ^{16}O* is the most favored at $\theta_\alpha=20°$ and $\phi_\alpha=0°$. For the O-α case, in which α decays of ^{20}Ne* contribute as the main process at small θ_α, similar kinematical conditions are found to hold.

In the inclusive measurement of HI's at 88 MeV presented in the preceding paper,[1] the few- and multinucleon-transfer reactions are mainly of DIC, which results in the forward peaking and even in the negative-angle deflection. The angular distributions

$$d^2\sigma/d\Omega\, dQ \propto \exp-(\mu\theta)/\sin\theta$$

and the Q_{gg} dependence of isotope production cross sections are consistent with the interpretation of the formation and the subsequential decay of the dinucleus system, DNS, except at very forward angles, say, $\theta_{HI}\lesssim 20°$. At extremely forward angles, other reaction mechanisms, such as projectile breakup, were already suggested.

In the present study, for $\theta_{HI}=20°$, α particles coincident with HI are concentrated at $\theta_\alpha\simeq-(10°-20°)$ or $\theta_\alpha=(10°-20°)$, $\phi_\alpha=0°$. Tsang

TABLE II. Relative energies $E_{O\text{-}\alpha}$ and resultant excitation energies E_x of intermediate projectilelike states in $^{16}O+^{27}Al\rightarrow{}^{20}Ne^*\rightarrow{}^{16}O(g.s.)+\alpha+{}^{23}Na(g.s.)$.

$E_{O\text{-}\alpha}$ (MeV)	E_x (^{20}Ne) (MeV)
4.0	8.7
7.3	12.0
10.5	15.2

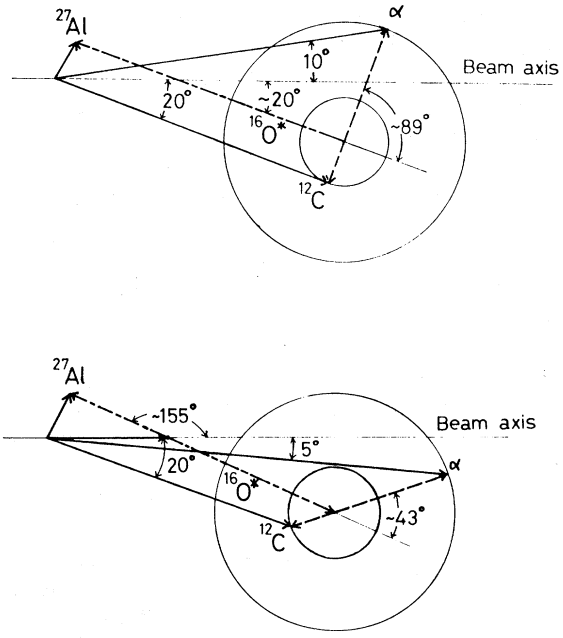

FIG. 13. Velocity diagrams for the reactions given by Eq. (8). The upper figure corresponds to the cases of $\theta_\alpha=10°$ and $\phi_\alpha=0°$, and the lower to that of $\theta_\alpha=5°$ and $\phi_\alpha=180°$.

et al.[6] showed that at 65 MeV, $\theta_C=30°$, the preequilibrium α-particle cross sections have a peak at $\theta_\alpha \simeq -20°$. The kinematical consideration mentioned above for the breakup of a projectilelike nucleus was experimentally verified. In contrast, for $\theta_{HI}=30°$, Fig. 3 shows no preferential direction of α particles coincident with HI. Indeed, a rotating $^{31}P^*$, for instance, would emit α particles with no preferential direction. This is the case with the present results at $\theta_{HI}=30°$ and the results of Harris *et al.*[5] at 100 MeV and at $\theta_{HI}=30°$. Moreover, Fig. 3 shows that the ratios of yields of HI at $\theta_{HI}=30°$ coincident with α particles to singles yields decrease as compared with those at $\theta_{HI}=20°$. This fact is interpreted to be due to the decrease of the contribution from the sequential α decay of projectilelike fragments with the increase of θ_{HI}.

The main reason for the differences and similarities between the observations of Harris *et al.*[4] and of Tsang *et al.*[6] at 65 MeV and $\theta_C=30°$, and of our present study at 87.4 MeV and $\theta_{HI}=20°$ and 30°, are thus understood to be due to: (a) the opening of a nonfusion reaction mechanism, i.e., DIC at $E_{lab} \gtrsim 65$ MeV; (b) the importance of the contribution from the breakup of projectilelike fragments at forward angles; and (c) the choice of favorable kinematical conditions.

From the results of Harris *et al.*[4] the angular distribution of α particles emitted from $^{31}P^*$ ($E_x \simeq 14.5$ MeV) shows the maximum at $\theta_\alpha^R=90°$ in the center of mass system of $^{31}P^*$. In the present case, if the α particles are emitted from $^{31}P^*$ and have a similar angular distribution, the coincident yield should be large at $\theta_\alpha \simeq (50°-55°)$ and $\phi_\alpha=0°$. In this region, the spectrum of $E_{\alpha\text{-Al}}$ of Fig. 10 shows the maximum at $E_{\alpha\text{-Al}} \simeq 6.5$ MeV and the peak position does not change for different θ_α. This suggests the occurrence of sequential α decay of $^{31}P^*$ even in the present work at large θ_α. Conversely, Tsang *et al.*[6] observed, even at a low energy of 65 MeV, a small fraction of the contribution of α particles from the breakup of $^{16}O^*$.

The reason why the sequential decays of α particles from the projectilelike fragments are enhanced for $E_{lab}=87.4$ Mev at $\theta_{HI}=20°$ can be also explained by the following favorable angular momentum matching conditions, which will give at least a necessary condition.

The values of the critical angular momentum L_{cr}, which limit the fusion cross section, are deduced from the experimental fusion cross sections for the $^{16}O+^{27}Al$ system[8] using the semiclassical approximation

$$\sigma_{fus}=\frac{\pi\hbar^2}{2\mu E_{c.m.}}(L_{cr}+1)^2 .$$

The closed circles in Fig. 14 are these results assuming $L_{cr}=J_{cr}$, where J_{cr} is the critical angular momentum of the compound states. The calculated L_{cr} is also shown in Fig. 14 depending on the region of the incident energies, as is described subsequently. The L_{cr} is identical to the fusion-barrier-top angular momentum of the entrance channel L_i for $E_{lab} \lesssim 60$ MeV; $L_{cr}=L_i$. On the contrary, above this energy, the L_{cr} is rather determined by the "statistical yrast line"[11] of the compound nucleus, J_y^{st}; $L_{cr} \simeq J_y^{st}$. It is quite clear that the DIC then becomes dominant in the angular momentum window of the entrance channel, $\Delta J=L_i-J_y^{st}$. Once the intermediate composite system is formed with spin J and after energy damping, it decays into a certain outgoing channel with a channel spin I and orbital angular momentum L_f such that $\vec{J}=\vec{L}_f+\vec{I}$. For a given L, L_i, or L_f, the barrier height of B_J must then be determined

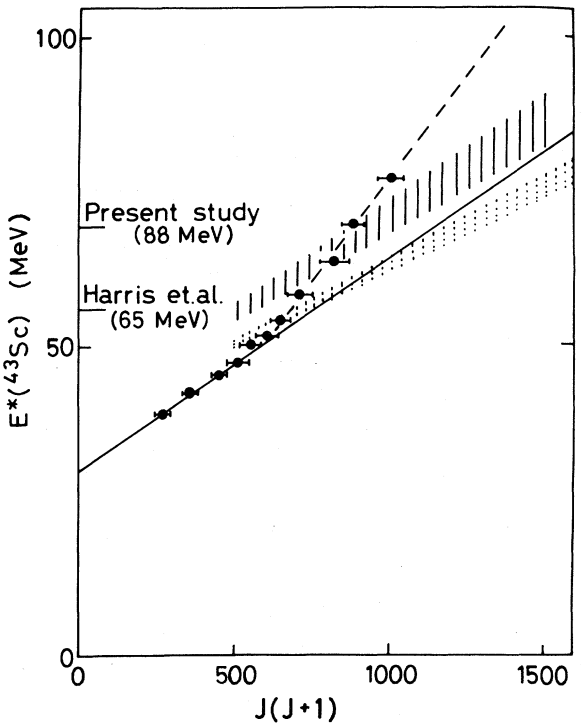

FIG. 14. Schematic representation of the angular momentum window for $^{16}O^*+^{27}Al$ and $^{31}P^*+^{12}C$ outgoing channels. Closed circles and error bars are L_{cr} deduced from the fusion data in Ref. 7, assuming $L_{cr}=J_{cr}$. The solid and dashed sloping lines are the calculated L_i and J_y^{st} lines, respectively (see the text). The area indicated with vertical solid lines is L_f for $^{16}O^*+^{27}Al$ for the range of excitation energies in E_x (^{16}O)=11.53 (2^+)–16.23 (6^+), and the area indicated with the vertical dashed lines is the range of L_f for $^{31}P^*+^{12}C$, with E_x (^{31}P)=14.5 for $I=\frac{17}{2}$ to $\frac{19}{2}$.

as follows:

$$B_J(L,\epsilon)=L(L+1)\hbar^2/2\mu R_B{}^2+\epsilon\ , \tag{9}$$

where

$$\epsilon=V_B(R_B)+E_B\ ,$$

$$V_B(R_B)=V_{\rm Coul}(R_B)+V_N(R_B)\ ,$$

and

$$R_B=r_B(A_1{}^{1/3}+A_2{}^{1/3})\ .$$

E_B is the Q value to form the compound nucleus or the composite system through the entrance or exit channel. By using the data and the relation

$$\sigma_{\rm fus}=\pi R_B{}^2(1-V_B/E_{\rm c.m.})$$

in the entrance channel for $E_{\rm lab}\lesssim 60$ MeV, we get[7] $r_B=1.45$ fm and $V_N(R_B)=-2.94$ MeV.

For the decay of the composite system the determination of the lowest barrier height is significant. Thus B_J is determined by the lowest $L_f=J-I$ as

$$B_J(J-I,\epsilon)=(J-I)(J-I+1)\hbar^2/2\pi R_B{}^2+\epsilon\ . \tag{10}$$

The bands of L_f lines for exit channels are calculated by using Eq. (10), since L_f with the lowest barrier is expected to be enhanced. Here, the values of r_B and $V_N(R_B)$ obtained from the entrance channel are used. In Fig. 14 are shown the band of L_f lines for ^{27}Al+^{16}O* [$E_x=11.53$ (2^+), 11.63 (3^-), and 16.23 (6^+)] together with those for ^{12}C+^{31}P* ($E_x\simeq 14.5$ MeV), assuming some high spin states such as $I=\frac{17}{2}$ or $\frac{19}{2}$ estimated approximately from the yrast line of ^{31}P. From this figure, it is fairly well shown why ^{27}Al+^{16}O* can be enhanced at $E_{\rm lab}=87.4$ MeV, but ^{31}P*+^{12}C at 65 MeV. Furthermore, it should also be mentioned that the above three excited states of ^{16}O* have a large $^{12}C_{gr}$-α cluster width.[10]

V. CONCLUSION

The reaction mechanisms of deep inelastic reactions in ^{16}O+^{27}Al collisions at 87.4 MeV were investigated using a HI-α-particle coincidence technique. Alpha particles were detected in coincidence with heavy ions detected at $\theta_{\rm HI}=20°$ and 30°.

In the in-plane coincidence measurement at $\theta_{\rm HI}=20°$, particles are emitted preferentially at $\theta_\alpha=-(10°-20°)$. At $\theta_{\rm HI}=30°$, in contrast, no preferential direction of α particles is observed. From the out-of-plane coincidence measurement, large amounts of α multiplicity are observed for HI=O, N, C, and B.

For $\theta_{\rm HI}=20°$, both for C-α and O-α correlations, the sequential α decays of projectilelike fragments were clearly identified. In the C-α case, in contrast to the conclusion of Harris *et al.* that the reaction proceeds via sequential α decays of intermediate ^{31}P* states, we found clear evidence of the sequential α decay of projectile nucleus ^{16}O*. Due to an improvement of energy resolution in this experiment, we could identify the intermediate states of ^{16}O* at $E_x\simeq 10$, 11.6, 13.2, 15.2, 16.2, and 21 MeV. Also in the case of O-α with $\theta_{\rm HI}=20°$, strong evidence of the sequential α decay of excited ^{20}Ne* at $E_x\simeq 8.7$, 12.0, and 15.2 MeV was obtained. At $\theta_{\rm HI}=30°$, in contrast, the sequential α decay of ^{31}P* may be the main process.

ACKNOWLEDGMENTS

The authors would like to thank Dr. K. Katori, Dr. T. Nomura, Dr. T. Matsuse, and Dr. T. Kishimoto for helpful discussions and also the technical staff at the Tandem Accelerator Center, the University of Tsukuba. This work was supported in part by the Nuclear and Solid State Research Project, University of Tsukuba.

[1]M. Sato, M. Sasagase, Y. Nagashima, J. Schimizu, T. Nakagawa, Y. Fukuchi, and T. Mikumo, Phys. Rev. C 27, 2621 (1983); see also T. Mikumo, M. Sasagase, M. Sato, T. Ooi, Y. Higashi, Y. Nagashima, and M. Yamanouchi, *ibid.* 21, 620 (1980).

[2]See, for example, H. Ho, R. Albrecht, W. Dünnweber, G. Graw, S. G. Steadman, J. P. Wurm, D. Disdier, V. Rauch, and F. Scheibling, Z. Phys. A 283, 235 (1977); C. K. Gelbke, M. Bini, C. Olmer, D. L. Hendrie, J. L. Laville, J. Mahoney, M. C. Mermaz, D. K. Scott, and H. H. Wieman, Phys. Lett. 71B, 83 (1977); T. Shimoda, M. Ishihara, H. Kamitsubo, T. Motobayashi, and T. Fukuda, in Proceedings of the IPCR Symposium on Macroscopic Features of Heavy Ion Collisions and Pre-equilibrium Process, Hakone, 1977, IPCR Cyclotron Report Suppl. 6, p. 400; R. K. Bowmik, E. C. Pollacco, N. E. Sanderson, J. B. A. England, and G. C. Morrison, Phys. Lett. 80B, 41 (1978); T. Fukuda, M. Ishihara, M. Tanaka, I. Miura, H. Ogata, and H. Kamitsubo, *ibid.* 99B, 317 (1981); Phys. Rev. C 25, 2464 (1982).

[3]D. H. E. Gross and J. Wilczyński, Phys. Lett. 67B, 1 (1977); P.-A. Gottschalk and M. Weström, Phys. Rev. Lett. 39, 1250 (1977); J. P. Bondorf and W. Nörenberg, Phys. Lett. 44B, 487 (1973).

[4]J. W. Harris, T. M. Cormier, D. F. Geesaman, L. L. Lee,

Jr., R. L. McGrath, and J. P. Wurm, Phys. Rev. Lett. 38, 1460 (1977).

[5]J. W. Harris, P. Braun-Münzinger, T. M. Cormier, D. F. Geesaman, L. L. Lee, Jr., R. L. McGrath, and J. P. Wurm, *Proceedings of the International Conference on Nuclear Structure, Tokyo, 1977,* edited by T. Marumori (Physical Society of Japan, Tokyo, 1978), p. 698.

[6]M. B. Tsang, W. G. Lynch, R. J. Puigh, R. Vandenbosch, and A. G. Seamster, Phys. Rev. C 23, 1560 (1981).

[7]B. B. Back, R. R. Betts, C. Gaarde, J. S. Larsen, E. Michelsen, and T. Kuang-Hsi, Nucl. Phys. A285, 317 (1977); R. Rascher, W. F. J. Müller, and K. P. Lieb, Phys. Rev. C 20, 1028 (1979).

[8]S. M. Lee., Y. Higashi, Y. Nagashima, S. Hanashima, M. Sato, H. Yamaguchi, M. Yamanouchi, and T. Matsuse, Phys. Lett. 98B, 418 (1981).

[9]T. M. Cormier, A. J. Lazzarini, M. A. Neuhausen, A. Sperduto, K. Van Bibber, F. Vidabaek, G. Young, E. B. Blum, L. Herreid, and W. Thoms. Phys. Rev. C 13, 682 (1976).

[10]Y. Suzuki, Prog. Theor. Phys. 56, 111 (1976).

[11]S. M. Lee, T. Matsuse, and A. Arima, Phys. Rev. Lett. 45, 165 (1980).